A Numerical Analysis of a High Temperature Solar Collecting Tube, Using Helium as an Heat Transfer Fluid

Luca Massidda
Researcher
Renewable Energies Program
CRS4
Pula, Italy 09010
Email: lucam@crs4.it

Alberto Varone
Researcher
Renewable Energies Program
CRS4
Pula, Italy 09010
Email: alberto@crs4.it

The Concentrating Solar Power (CSP), and parabolic trough in particular, may provide a possible solution to global energy problem within a relatively short time frame, by reducing the actual Levelized Energy Cost in the medium and long term. The use of gases as an heat transfer fluid may give interesting development to this technology, allowing to reach higher operating temperatures and power conversion efficiencies; the use of gas may be cheap and safe and does not demand for excessive modification on the existing technology. This article analyses the problems connected to the absorber tube, which is the most critical part of the system, and the element that may be subject to the most severe consequences due to the use of a gas as a heat transfer fluid. The fluid dynamics of the gas in the pipe, the heat-transfer in the system and the stresses and deformations of the pipe structure have been simulated numerically. The resulting flow characteristics, temperature distributions and stresses for a reference test case are discussed, and some possible solutions to enhance the system performance are analyzed.

1 Introduction

The use of several gases as a heat transfer fluid will be analyzed in detail in a recently approved research program in Italy, with the aim to experiment new solutions to increase the efficiency of the trough solar power plant.

The traditional SEGS type trough plants adopt a synthetic oil as a heat transfer fluid, but the maximum fluid temperature is limited to $400°C$, due to the thermal stability of the oils, although higher temperatures would lead to higher power conversion efficiencies [1]. A recent enhancement of this concept is represented by the DSG type cycle (Direct Steam Generation), in which water is used as an heat transfer fluid, and the steam is directly generated inside the absorber tube at very high pressures and sent directly to the power block, without the need for a heat exchanger [2]. The limit on the maximum temperature appears to be partly related to the stability of the absorbance coating of the tube at temperatures higher than $440°C$. Higher temperatures are envisaged in the ENEA trough concepts, which use molten salt in the absorber tube [3]. The molten salt circuit may reach a maximum temperature of $550°C$. A newly developed Heat Collecting Element (HCE) is designed to match these operating conditions with an absorbance layer that has very low emissivity up to $580°C$ [4].

Gases do not put any limitation on the maximum outlet temperature of the system; this value would be related to the performance and structural limits of the heat collecting element and not to the fluid properties. Some difficulties are anyway envisaged, since the heat capacity of gases is lower than the other fluids adopted so far, and lower heat transfer between fluid and pipe internal surface are expected as well; high pressures and high fluid velocities are therefore required. A significant thermal gradient is expected in the steel tube of the HCE and the maximum temperature of the tube should be an important factor to be considered as well [5].

This paper describes the numerical simulation of the fluid dynamics and of the thermal and structural performance of a trough line when a gas is used as a heat transfer fluid, using an ENEA-like HCE. The system is studied using Computational Fluid Dynamics (CFD) and Finite Element Method (FEM) numerical methods.

2 System description

The heat collecting element basically consist of a stainless steel tube, in which the heat transfer fluid flows, covered on the external surface by a solar-selective and low-emissive absorbance layer. The tube is insulated and protected from oxydation by an external glass tube; moreover vacuum is produced between the steel and glass tube, thus the convection heat transfer is inhibited and the heat losses are mainly radiative [1].

The solar radiation is reflected on the HCE by a system of parabolic mirrors, as usual in the trough scheme; the characteristics of the system used as a reference are reported in table 1.

Table 1. Characteristics of the investigated system

Mirror width	5.75	m
Trough length	97.44	m
Focal length	1.71	m
Steel tube int. diameter	64	mm
Steel tube ext. diameter	70	mm
Glass tube int. diameter	109	mm
Glass tube ext. diameter	115	mm
Tube length	4060	mm
Inlet temperature	150	°C
Outlet temperature	460	°C
Solar irradiation on mirror	900	W/m2
Mirror efficiency	0.79	%
Total collected sun radiation	408.8	kW

The system performances have been first analyzed by a simplified model, making simple heat balance and pressure drop calculations along the trough line [6]. The results for several gases are shown in table 2.

A monodimensional model is anyway non satisfactory, due to the simplifications in the physics, but also due to the non uniform irradiation and heating of the tube surface. The temperature distribution in a section of the tube and of the fluid inside is not axi-symmetric, a temperature gradient is generated with higher temperatures on the irradiated zone. This gradient limits the maximum fluid temperature that may be achieved and may cause severe stresses on the tube.

It appeared that a further investigation is required for the fluid dynamics and for the heat transfer problem.

3 CFD simulations

A three dimensional fluid dynamical and thermal analysis on both the fluid and the solid phase has been run by means of the Computational Fluid Dynamics code FLUENT. The analysis has been focused on the fluid and on the steel pipe; the trough line is composed by 24 heat collecting elements, each 4.060m long for a total trough line length of 97.44m.

The results of the simplified model have been used to provide the approximate value for some boundary conditions of the analysis, such as the inlet temperature and velocity, and the outlet pressure of the gas.

The model is restricted to the fluid inside the tube and to the steel tube; the glass tube is not included. The detail of the tube suspensions for the support structure and the connections between the steel and glass tubes among others, are neglected in the analysis for the sake of simplicity.

The absorbed solar radiation is modeled using the heat flux distribution of previous ray tracing calculations [3].

The analysis is restricted to Helium at reference conditions: the temperature of the fluid at the initial section of the trough line is fixed at 150°C and the pressure at the end of the trough line is 20bar. The mass flow rate is calculated to have an average fluid outlet temperature of 460°C.

The values of the maximum temperature in the tube and the temperature gradient in a tube section are important factors for the technical feasibility of the system, for the stability of the absorbing coating and the strength of the glass and steel tubes.

Since the temperature values and distribution for a given outlet temperature of the fluid are influenced by the heat exchange coefficient at the pipe internal surface, it is therefore interesting to enhance the heat transmission to reduce the maximum temperature, and to have more uniform temperature in the steel tube and in the fluid, for any section considered.

Two simple ways to enhance the heat transmission are analyzed: the increase in the surface roughness and the use of helical swirl generators [7, 8].

The internal surface roughness enhances the fluid turbulence, increasing the heat exchange inside the fluid and between the fluid and the tube surface. The performances of a smooth tube are compared to two systems having a surface roughness of 0.1mm and 0.25mm.
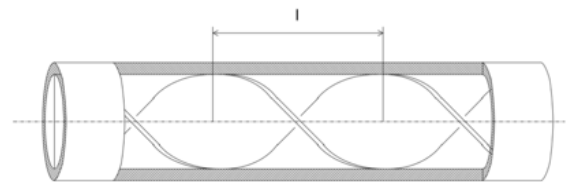

Fig. 1. Sketch of the absorber tube with the swirl tape insert

The helical swirl generators are steel tapes, twisted and inserted in the steel tube. Their function is not only to increase the fluid turbulence, but also to refresh the fluid stream in contact with the hot portion of the tube surface and avoid a stratified flow (see Fig. 1). Three systems with different swirl tape length of 8.120m, 4.060m and 2.030m, are studied and compared to the performances of a regular smooth tube.

3.1 Meshes

Several meshes at different levels of refinement have been tested. Due to the very stretched aspect ratio of the geometry (7cm external diameter, 97.44m long) a mixed structured-unstructured mesh was used. Structured meshes

	H2	He	CO2	N2	Air	
Mass flow rate	0.087	0.243	1.193	1.154	1.181	kg/s
Inlet temperature	152	152	152	152	152	°C
Outlet temperature	467	467	460	467	467	°C
Inlet pressure	20	20	20	20	20	bar
Pressure loss	0.111	0.442	0.687	1.047	1.069	bar
Fluid velocity at the outlet	39.2	58.5	26.2	41.0	40.8	m/s
Esteemed power to the fluid	387.7	387.6	385.8	385.7	385.7	kW

Table 2. Characteristics of the investigated system

were used for the near-wall fluid region and for solid layers in the transversal plane.

The same mesh was used in all the analyses with and without the presence of the helical tape. The volume of the fluid is divided in two parts separated by a surface; this surface is considered as an internal boundary when no helical tape is present, and as an internal surface when the tape is considered. The mesh is refined near the surface to solve for the boundary layer.

The mesh has an extruded cylindrical shape; the number of swirls considered is so low that the influence of the tangential velocity of the fluid could be neglected. The effect of the fluid swirl has been simulated rotating the heat flux source around the tube axis along the length, as discussed in the following.

3.2 Material properties

The properties of the AISI 316 stainless steel used for the heat collecting tube are listed in table 3. The gas is governed by to the ideal gas law with viscosity and thermal conductivity function of the temperature [9].

The ideal gas approximation is acceptable for Helium at the operating conditions; the values of dynamic viscosity and thermal conductivity are variable with temperature according to the following laws (with T in K): [10]

Viscosity $(kg/m/s)$: $\mu = 6.9847 \cdot 10^{-6} + 4.5517 \cdot 10^{-8}T - 6.162 \cdot 10^{-12}T^2$

Thermal conductivity $(W/m/K)$: $k = 0.054615 + 0.0003556T - 4.8326 \cdot 10^{-8}T^2$

3.3 Collector irradiation

The concentrated solar irradiation is simulated through a volumetric heat source applied to the first layer of cells near the illuminated surface. The distribution of the solar irradiation concentrated on the pipe surface results from a ray tracing analysis and is shown in Fig. 2 [3].

In order to simulate the effect of a swirling tape, we simplified the computational problem adopting a straight, not swirled mesh, and rotating the heat flux around the tube axis instead. In this way we are neglecting the tangential component of velocities and acceleration, this may be an acceptable approximation if the tangential velocity magnitude is low when compared to the axial component, as it happens with a low number of tape turns per tube length.

The angle α in the previous expressions is calculated as a function of the point position. If ϕ is the angle of the point around the pipe axis, z is the axial coordinate and l is the tape
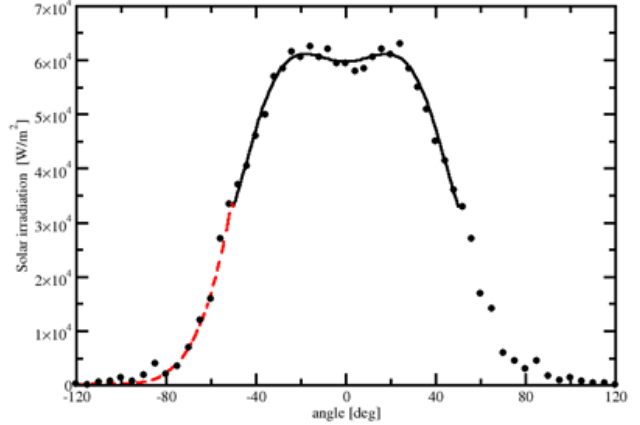

Fig. 2. Solar irradiation on the pipe external surface and interpolation curves resulting from a ray tracing numerical simulation

length required for a flow inversion (see Fig. 1), then α may be calculated as:

$$\alpha = \phi + \pi\frac{z}{l} \qquad (1)$$

When the swirling tape is not included, the angle α is simply taken as equal to ϕ.

3.4 Thermal losses

The absorber tube is thermally insulated as well as possible. The convection is inhibited by the vacuum annulus between the steel tube and the external glass tube; the thermal irradiation is minimized by the use of specifically designed absorber coatings, that have low emissivity in the infrared range up to 580°C, but having high emissivity and absorptivity for the wavelengths of the solar spectrum.

It has been demonstrated [11] that the heat losses of and HCE can be modelled, with good agreement to the experimental results, by using the following simple expression:

$$q = (a+cV)(T_{ab}-T_a)+\varepsilon_{ab}b(T_{ab}^4-T_{sky}^4) \qquad (2)$$

where T_{ab} is the mean tube temperature, T_a is the air temperature, V is the wind velocity, and ε_{ab} is the emissivity of the HCE. The coefficients a, b and c, are relative to the heat conduction through the supports, to the convective losses from

Temp.	Density	Specific heat	Thermal conduct.	Elastic modulus	Thermal exp. coeff.	Yield stress	Allowable stress
K	kg/m3	J/kg/K	W/m/K	GPa	10-6/K	MPa	MPa
300	7960	468	13.40	194	15.2	207	110
400		504	15.20	188	16.1	167	110
500		527	16.75	182	16.9	143	110
600		550	18.30	174	17.5	129	110
700		563	19.80	166	17.9	121	110
800		571	21.30	158	18.3	118	105
900		589	22.75	149	18.6	113	68
1000		602	24.20	136	18.8	103	21

Table 3. AISI 316 stainless steel properties

the glass tube, and to the radiation losses; the latter term is by far the most important for high temperatures.

Therefore it appeared that for the limits of our analysis the heat losses of the pipe could be modelled with reasonable accuracy by applying a heat sink to the external layer of cells of the model. The heat flux is simply calculated as:

$$q = \varepsilon_{ab} T_{ab}^4 \qquad (3)$$

where T_{ab} is the surface temperature, σ is the Stefan-Boltzmann constant and ε_{ab} is the infrared emissivity, assumed equal to 0.16, higher than the value obtained in the ENEA HCE system [4]. This expression seems to fit reasonably well also with recent field measurements [12].

3.5 Solution algorithm

The fluid equations, solved for steady flows, are computed using the segregated solver method. Using this approach, the governing equations are solved sequentially. Since the governing equations are non-linear (and coupled), several iterations of the solution loop must be performed before a converged solution is obtained. Since the flow is always turbulent, several turbulence models have been checked; the $k - \varepsilon$ model resulted to give the most satisfactory results.

4 CFD results

4.1 Smooth tube

The results for the Helium at 20bar and initial temperature of 150°C, are shown first for the smooth pipe; Figure 3 shows the temperature contours plot for three different sections (at inlet, middle and outlet sections).

The temperature distribution in the steel and gas section is influenced by the distribution of the solar radiation on the tube external surface, by the heat transfer coefficient on the internal surface and by the thermal conductivity of the steel. The maximum temperature of the steel reaches 550°C at the end of the line, the temperature difference between enlightened and non-enlightened areas of the tube is almost constant along the trough line and higher than 100°C. Similar results are obtained in numerical simulations for the final portion of the DSG trough line [13]. The thermal gradient is much lower in systems where slower and denser fluids

such as molten salt or mineral oils, are used as thermal carriers [3, 14].

The thermal gradient in the tube surface induces into the gas two big recirculation cells, but the resulting transversal velocities are several orders of magnitude lower than the longitudinal velocity and have a limited effect on the heat transmission between the steel tube and the fluid.

4.2 Rough tube

The turbulent heat transfer coefficient inside the tube may be enhanced to reduce the temperatures differences; a more turbulent flow may be obtained using rough internal surfaces tubes instead of smooth tube. As a drawback, an increase of the pressure loss is expected and an higher pumping power is required.

Table 4 shows a performance comparison between smooth and rough tubes.

The surface roughness does not have a significant effect on the velocity profile, the pressure drop is increased along the pipe length, and the most significant effect is the reduction of the tube temperature peak, related to the increased heat transfer coefficient.
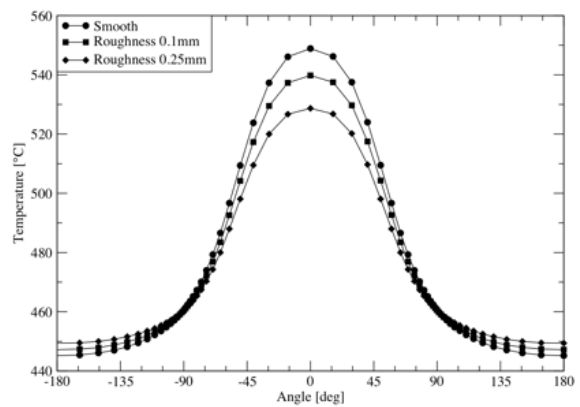

Fig. 4. Temperature distribution on the tube external surface at the outlet section of the trough line for several values of the surface roughness
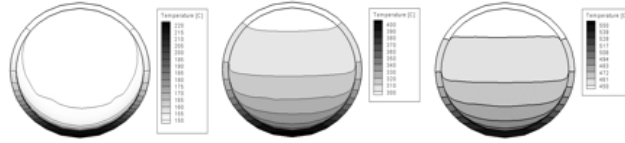
Fig. 3. Temperature distribution in three sections (inlet, middle and outlet) for a smooth tube with Helium at 20bar

Table 4. Flow results for Helium for smooth and rough tubes

Roughness	Smooth	0.1	0.25	mm
Mass flow rate	0.2152	0.2152	0.2152	kg/s
Inlet pressure	20.0	20.0	20.0	bar
Inlet average velocity	30.50	30.4	30.2	m/s
Inlet temperature	150	150	150	°C
Outlet pressure	19.63	19.55	19.44	bar
Outlet average velocity	53.6	53.7	53.7	m/s
Outlet average temperature	461.2	461.8	462.7	°C
Outlet steel minimum temperature	443.9	445.9	448.1	°C
Outlet steel maximum temperature	548.3	539.1	528.1	°C
Pressure drop	0.37	0.45	0.56	bar
Pumping power ($\eta_c = 0.8$)	4.40	5.37	6.71	kW

The temperature distribution on the external tube surface at the final section is shown in Fig. 4. The temperature gradient in the final section is reduced from 105°C for the smooth tube to 80°C for a tube having a surface roughness of 0.25mm. The lower thermal gradient results in lower stresses in the steel tube, and the lower value of the maximum temperature in the steel would allow also an increase in the fluid outlet temperature. The price to be paid is an increase in the pumping power required, but still low if compared to power extracted.

4.3 Swirl tapes

The thermal gradient on the pipe may be reduced by adopting twisted tape inserts that would swirl the gas inside the tube, enhancing the fluid turbulence and the heat transfer coefficient, and also refreshing the fluid stream in contact with the hot portion of the internal surface. The internal surface of the tube and tape are smooth but additional boundary layers have origin on the tape surfaces, increasing the turbulence of the flow. An increase in the pressure drop with respect to the smooth tube is expected, too.

The thickness of the tape is neglected and the surface is assumed adiabatic. The swirl length of the tape insert is defined as the length required for a flow inversion, or a turn of the flow of 180°; three swirl lengths are considered (8.120m, 4.060m and 2.030m) that correspond to a complete flow turn every four, two and a single tube module. The results, also compared to the smooth tube, are listed in table 5.

Figure 5 shows the temperature distribution on the tube external surface, at the output section, for several values of the swirl length. The swirl tape has a positive effect on the thermal gradient of the section; the effect of the swirl length is evident but the overall effect is limited; it might be necessary to increase the swirl effect with a further reduction of the swirl length, but this might lead to an increase of the
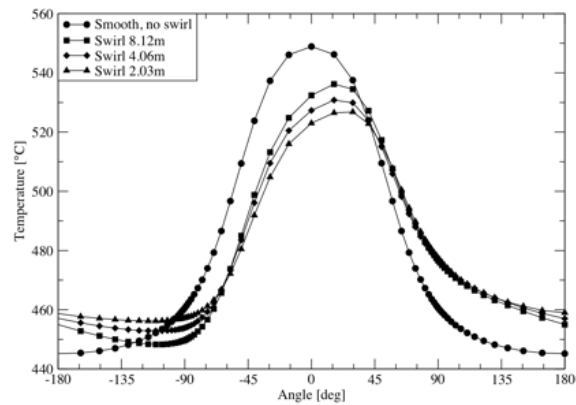

Fig. 5. Temperature distribution on the tube external surface at the outlet section of the trough line for several values of the swirl length

pressure drop. The temperature difference is reduced from 105°C for the smooth tube to a minimum of 71°C for a tube having a swirl length of 2.030m.

4.4 Enhanced tube

Finally we compare the standard smooth tube with an enhanced tube that has both a helical tape with swirl length of 2.030m and a surface roughness of 0.25mm, see table 6. The two systems have the same boundary conditions and mass flow rate; the high value of the heat exchange coefficient in the enhanced tube reduces the temperature gradient in the steel tube section and between the tube and the fluid, thus permitting higher fluid outlet temperature values.

The Fig. 6 and 7 show the temperature distribution on

Table 5. Flow results for Helium with several helical tape inserts

| Swirl lenght	No swirl	8120	4060	2030	mm
Mass flow rate	0.2152	0.2152	0.2152	0.2152	kg/s
Inlet pressure	20.0	20.0	20.0	20.0	bar
Inlet average velocity	30.50	29.96	29.96	29.96	m/s
Inlet temperature	150	150	150	150	°C
Outlet pressure	19.63	19.38	19.37	19.37	bar
Outlet average velocity	53.6	52.67	52.68	52.68	m/s
Outlet average temperature	461.2	460.9	461.1	461.1	m/s
Outlet steel minimum temperature	443.9	448.3	452.9	456.2	°C
Outlet steel maximum temperature	548.3	536.2	530.8	526.8	°C
Pressure drop	0.37	0.63	0.63	0.63	bar
Pumping power ($\eta_c = 0.8$)	4.40	7.57	7.57	7.57	kW
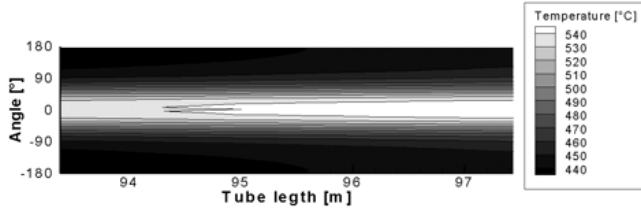
Fig. 6. Temperature on the external surface of the final module of the trough line. The tube is smooth and the fluid is Helium at 20bar
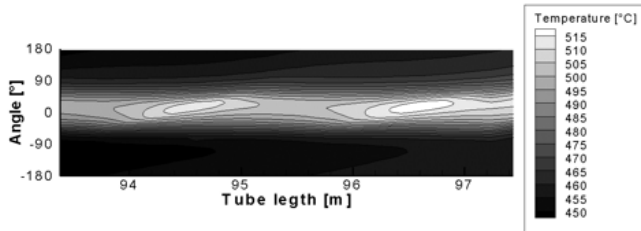

Fig. 7. Temperature on the external surface of the final module of the trough line. The tube has a surface roughness of 0.25mm and a swirl tape with inversion length of 2.03m is used. The fluid is Helium at 20bar

the external surface for the smooth tube and for the enhanced tube. As expected the internal surface roughness and the swirl tape have the effect to reduce the temperature gradient in the tube, that equals 54°C. The temperature profile of Fig. 7 is no longer symmetric, due to the swirl tape, moreover the maximum temperature is not reached in the outlet section.

5 Structural analysis

The stresses and strains of the steel tube have been analyzed by means of a finite element modeling; the analysis has been focused on the final pipe of the trough line where the maximum temperatures are found. Apart from the internal pressure of 20bar and the self weight, that are constant for the entire trough line, we applied the temperature distribu-

tion previously calculated in the CFD analysis for a smooth pipe for which the surface roughness is equal to zero and the enhanced tube that has a mean surface roughness of 0.25mm and an helical tape with swirl length of 2.030m.

We used ANSYS, the model is formed by 2880 brick elements and 16416 nodes. We run both linear and nonlinear static structural analyses, with material properties variable with temperature.

The tube is supposed to be entirely made from a AISI 316 stainless steel, the material properties are listed in the table 3, the maximum allowable stress for 20 years of operating lifetime is taken from the ASME NCC boiler and Pressure Vessel code.

The boundary conditions at the end section of the tube are chosen to approximate the effect of a long trough line on the portion considered. The tube may expand freely in the radial and axial directions but the two end section can not move or rotate in any transverse direction, due to the pipe supports and to the symmetry boundaries of the trough line.

5.1 Results

Figures 8 and 9 show the equivalent stresses (according to the Guest-Tresca stress criterion) on the external surface of the steel tube as calculated by the linear elastic analysis for the smooth and for the enhanced tube. The stresses on the internal surfaces have a similar distribution and values. The stresses are very high, and in both tube configurations would cause the yielding of the steel: the maximum value of the equivalent stress in an elastic analysis reaches the maximum value of 230MPa in the smooth tube, whereas in the enhanced tube the maximum stress is reduced to 150MPa due to the lower thermal gradients.

On the final portion of the pipe line the maximum temperature found is 600°C, at this temperature the yield stress is 113MPa, and the maximum allowable stress is 68MPa.

The mechanical stresses are due to the superposition of the loads acting on the pipe and are mainly due to the internal pressure and to the thermal stresses, the latter having higher values but being much less dangerous than the pressure load. Thermal stresses are in fact self-limited, they act as a prescribed displacement for the structure: if the structure yields to reach the required deformation no further plastic deformation would occur. On the contrary, pressure loads are not self-limited: if the pipe yields due to internal pressure, or to

Table 6.   Smooth and "enhanced" tube performance comparison

	Smooth tube		
Roughness	Smooth tube	0.25	mm
Swirl length	No swirl	2030	mm
Mass flow rate	0.2152	0.2152	kg/s
Inlet pressure	20	20	bar
Inlet average velocity	30.50	30.20	m/s
Inlet temperature	150	150	°C
Outlet pressure	19.63	19.56	bar
Outlet average velocity	53.6	53.72	m/s
Outlet average temperature	461.2	462.4	°C
Outlet steel minimum temperature	443.9	457.5	°C
Outlet steel maximum temperature	548.3	511.3	°C
Pressure drop	0.37	0.84	bar
Pumping power ($\eta_c = 0.8$)	4.40	9.93	kW
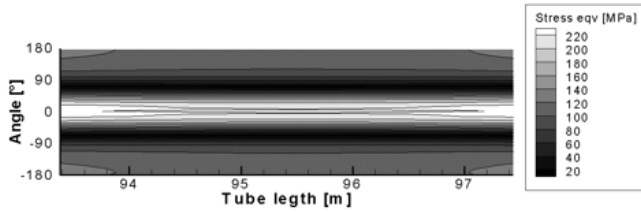
Fig. 8.   Equivalent stresses on the external surface for the last module of the trough line, resulting from an elastic analysis. The tube is smooth and the Helium pressure is 20bar
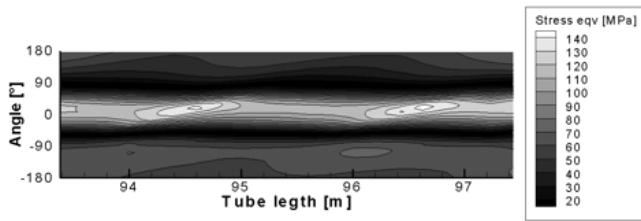

Fig. 9.   Equivalent stresses on the external surface for the last module of the trough line, resulting from an elastic analysis. The tube has a surface roughness of 0.25mm and a swirl tape with inversion length of 2.03m is used. The fluid is Helium at 20bar

gravity acting, reaches the operating temperature and the design pressure, and then returns to the initial condition, cycled several times.

Fig. 10.   Equivalent stresses on the external surface for the last module of the trough line. The result is calculated in a non-linear analysis when the maximum temperature is reached. The tube is smooth and the Helium pressure is 20bar
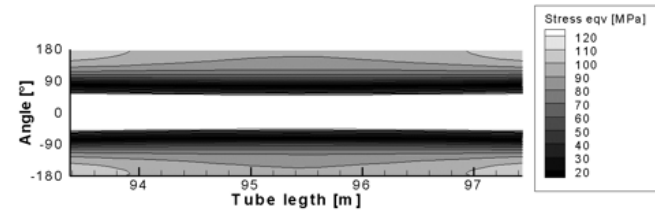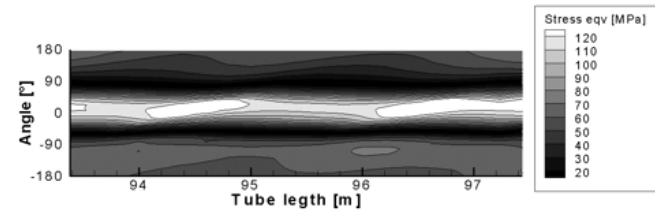

Fig. 11.   Equivalent stresses on the external surface for the last module of the trough line. The result is calculated in a non-linear analysis when the maximum temperature is reached. The tube has a surface roughness of 0.25mm and a swirl tape with inversion length of 2.03m is used. The fluid is Helium at 20bar

its self weight, the structure continues to deform plastically until the strain hardening of the material balances the applied load, or until the rupture of the material.

It is therefore important to identify the stresses due to the pressure and gravity loads only. It results that the stresses are mainly due to the pressure; the equivalent stress is almost uniform on the internal surface reaching the maximum value of 25MPa, much lower than the allowable stress limit.

The final part of both smooth and enhanced pipe has been further analyzed with a non-linear simulation. We adopted an elastic-perfectly plastic material model with bi-linear kinematic hardening law; the hardening module is set to zero. We simulated a repeated on-off cycle, in which the pipe starts at ambient temperature with only pressure and

It resulted that after the first cycle the stress pattern repeats over and over with no further plastic deformation. When the pipe reaches the operating condition the first time a plasticization occurs approximately in all the heated area
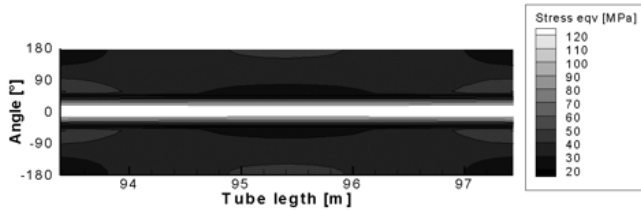
Fig. 12. Equivalent stresses on the external surface for the last module of the trough line. The result is calculated in a non-linear analysis when the minimum temperature is reached; the residual stresses due to the steel yielding are evident. The tube is smooth and the Helium pressure is 20bar

of the pipe as shown in Fig. 10 for the external surface of the smooth pipe and in Fig. 11 for the enhanced pipe.

When the pipe is cooled down the residual stresses appear for the smooth tube, as shown in Fig. 12 for the external surface; the maximum stress value is still close to 120MPa but in this case there is no further plastic deformation since the material yield stress at ambient temperature is much higher. The residual stresses in the enhanced tube are almost negligible, and the stresses in low temperature condition are only due to pressure and gravity.

The reduction of the temperature gradient in the pipe section, as observed in the comparison between the smooth and the enhanced pipe, greatly reduces the plastic deformation. The yielding is still present, and it is confined in a limited portion of the pipe surface; the plastic deformation is self limited as mentioned and will not grow in time with repeated cycles.
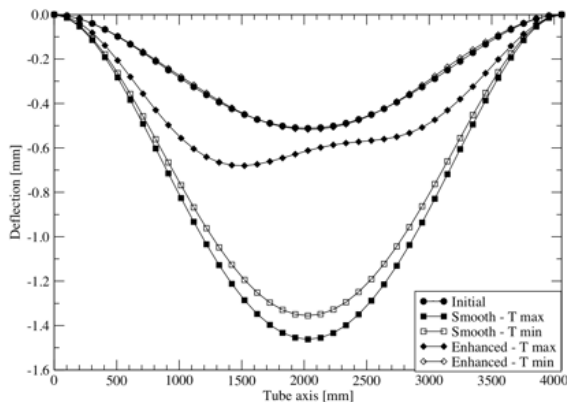

Fig. 13. Deformation of the axis of the last module of the trough line under a cycled thermal load, for a non-linear analysis and for the standard smooth and the enhanced tube (roughness 0.25mm and swirl length 2.03m)

In the Fig. 13 the deformation of the pipe axis is shown for the extreme conditions of the thermal cycle, and for the initial condition at ambient temperature in which no plastic deformation has occurred yet. The initial condition is equal for both tubes, the thermal deformation sums to the effect of the self-weight when the operating temperature is reached; the effect of the swirl on the temperature distribution is responsible for the particular deformation pattern. When the tube is cooled down the enhanced tube mostly recovers its initial position, since its deformation is mostly elastic. The smooth tube on the contrary is subject to a diffuse plasticization, with residual stresses causing the deformation in the minimum temperature condition.

6 Conclusions

The use of a gas as a heat transfer fluid for a trough solar collector has been analyzed by means of numerical simulations. This fluid is characterized by a low specific heat capacity and a low heat transfer coefficient, and relatively high values of the fluid pressure and the mass flow rate are required.

The performance of a system using helium has been analysed first using a standard heat collecting element, designed for a different fluid, and then showing the effects of an increase of the internal surface roughness and of the use of twisted tape swirl generators.

The structural analysis showed that the non-uniform thermal distribution on the pipe surface causes a severe stress condition on the steel pipe, which may affect its strength and performance. The loads due to pressure and self-weight appeared to be commensurate to the design of the pipe, but the thermal stresses resulted very high.

The use of heat transfer enhancements greatly improves the system performances by increasing the heat transfer coefficient and reducing the temperature gradient in the tube section. The reduction of thermal stresses is anyhow still not sufficient to avoid plastic deformations in the structure. New means to enhance turbulence and new system configurations, for instance with the use of a secondary reflector, may be analyzed in order to optimize the performances of the system.

References

[1] Price, H., Lupfert, E., Kearney, D., Zarza, E., Cohen, G., Gee, R., and Mahoney, R., 2002. "Advances in parabolic trough solar power technology". *Journal of Solar Energy Engineering,* **124**, pp. 109–125.

[2] Eck, M., Zarza, E., Eickhoff, M., Rheinlander, J., and Valenzuela, L., 2003. "Applied research concerning the direct steam generation in parabolic troughs". *Solar Energy,* **74**, pp. 341–351.

[3] Rubbia, C., 2001. Solar thermal energy production: guidelines and future programmes of enea. Tech. Rep. ENEA/TM/PRESS/2001-07, ENEA.

[4] Maccari, A., 2006. "Enea activities on csp technologies". In Parabolic Trough Technlogy Workshop, Incline Village, NV.

[5] Eck, M., and Steinmann, W. D., 2005. "Modelling and design of direct solar steam generating collector fields". *Journal of Solar Energy Engineering,* **127**, pp. 371–380.

[6] Murgia, G., Pili, P., and Varone, A., 2005. Calcoli termofluidodinamici del ricevitore e del sistema di stoccaggio di un impianto solare ad alta temperatura per la produzione di energia termica tramite concentratori parabolici lineari. Internal Note 05, CRS4.

[7] Eiamsa-ard, S., and Promvonge, P., 2005. "Enhancement of heat transfer in a tube with regularly-spaced helical tape swirl generators". *Solar Energy,* **78**, pp. 483–494.

[8] Thome, J. R., 2006. *Engineering Data Book III*. Wolverine Tube, Inc.

[9] Karditsas, P. J., and Baptiste, M.-J., 1995. Thermal and structural properties of fusion related materials. Report 294, UKAEA FUS.

[10] Incropera, F., and DeWitt, D., 1985. *Fundamentals of Heat and Mass Transfer*, 2nd ed. John Wiley.

[11] ODEH, S. D., MORRISON, G. L., and BEHNIA, M., 1998. "Modelling of parabolic trough direct steam generation solar collectors". *Solar Energy,* **62**(6), pp. 395–406.

[12] Price, H., Forristall, R., Wendelin, T., Lewandowski, A., Moss, T., and Gummo, C., 2006. Field survey of parabolic trough receiver thermal performance. Tech. rep., NREL.

[13] Benz, N., Eck, M., Kuckelkorn, T., and Uhlig, R., 2006. "Development of receivers for the dsg process". In 13th SolarPACES Internationa Symposium, Seville, Spain.

[14] Maciocco, L., 2001. Simulation of enea solar collector pipe using a binary mixture of molten nitrate salts. Internal Note 04, CRS4.